D18

Surface tension and contact angles: molecular origins and associated microstructure

H. T. Davis

Department of Chemical Engineering and Materials Science, University of Minnesota, 151 Amundson Hall, 421 Washington Avenue S.E., Minneapolis, Minnesota 55455

Abstract

Gradient theory converts the molecular theory of inhomogeneous fluid into nonlinear boundary value problems for density and stress distributions in fluid interfaces, contact line regions, nuclei and microdroplets, and other fluid microstructures. The relationship between the basic patterns of fluid phase behavior and the occurrence and stability of fluid microstructures is clearly established by the theory. All the inputs of the theory have molecular expressions which are computable from simple models.

On another level, the theory becomes a phenomenological framework in which the equation of state of homogeneous fluid and sets of influence parameters of inhomogeneous fluids are the inputs and the structures, stress tensions and contact angles of menisci are the outputs—outputs that find applications in the science and technology of drops and bubbles.

Introduction

As witnessed by the papers presented at this colloquium, drops and bubbles, thin films and adsorbed layers, and contact angles are key actors in numerous natural and man-made processes. With our knowledge of and demands on these processes becoming more sophisticated, it is increasingly important to have a molecular level theory of structure and stress in interfaces. Although the formal statistical mechanical theory of inhomogeneous fluids at equilibrium has been developed rather extensively over the last two decades, the formal theory is presently intractable.[1,2] Far more powerful is gradient theory,[2] an approximation going back to Rayleigh[3] and van der Waals[4] which was rediscovered by Cahn and Hilliard[5] and was recently put into modern form by Bongiorno *et al.*[6] and Yang *et al.*[7] Successes in predicting the surface tension of polymer melts,[8] hydrocarbons and their mixtures,[9] and water [10] prove that the theory is useful for real fluids. In this paper, I outline the elements of gradient theory and describe applications that my Minnesota colleagues and I have made of the theory to fluid-fluid interfaces, fluids at solid surfaces, and drops and bubbles.

Gradient theory of microstructured fluids

A fluid microstructure is an inhomogeneous region in a fluid in which component densities vary appreciably over molecular distances. Any fluid is, of course, inhomogeneous because of the presence of gravity. However, the inhomogeneities that result from gravity are so weak that component densities vary negligibly over molecular distances. Similarly, the inhomogeneities induced by ordinary centrifugal fields and by the temperature and composition gradients involved in the usual transport situations are very weak. If the component densities vary sufficiently little over molecular distances, then the thermodynamic functions can be approximated locally by the corresponding functions for homogeneous fluid at the local composition. In fluid microstructures the effect of the local component density variations must be accounted for in the local thermodynamic functions.

In the absence of external fields and density inhomogeneities, the Helmholtz free energy density is f_o. From intermolecular interactions species i and j give to f_o a contribution of the order of $a_{ij}n_in_j$, n_i and n_j being component densities and a_{ij} a characteristic energy parameter. The factor $1/2\ n_in_j$ is a measure of the number of interacting pairs. If the fluid is inhomogeneous at position $\underline{r}$, then the number of interacting pairs in the vicinity of $\underline{r}$ should be corrected by some amount $1/2\ \delta n_i\delta n_j$. An estimate of δn_i is $r_{ij}\nabla n_i$, r_{ij} the range of the intermolecular force between i and j and ∇n_i the gradient of n_i at $\underline{r}$. It follows heuristically then that the local Helmholtz free energy density of inhomogeneous fluid is $f_o(\underline{n}) + \sum_{i,j}^{\nu} \frac{1}{2} c_{ij}\nabla n_i\cdot\nabla n_j$ plus terms higher order in gradients of component densities; $f_o(\underline{n}(\underline{r}))$ is the Helmholtz free energy density of homogeneous fluid at the local composition $\underline{n}(\underline{r}) \equiv \{n_1(\underline{r}), n_2(\underline{r}), \cdots, n_\nu(\underline{r})\}$ and the terms involving density gradients are the Helmholtz free energy density of the inhomogeneity. The quantity c_{ij} is proportional to $a_{ij}r_{ij}^2$, the proportionality factor arising from appropriate molecular averaging. If an external conservative potential $u_e^i(\underline{r})$ is present, then to the local free energy density is added $\sum n_i u_e^i$. Putting together the pieces of this heuristic argument, one gets the gradient theoretical formula for the Helmholtz free energy F of inhomogeneous fluid:

$$F = \int_V [f_o(\underline{n}) + \sum_{i,j} \frac{1}{2} c_{ij} \nabla n_i \cdot \nabla n_j + \sum_i n_i u_e^i] d^3r \ . \qquad (1)$$

If the density gradients are macroscopic, e.g., caused by gravity or ordinary centrifugal fields, then ∇n_i is of the order of n_i/L, L being the dimension of the system. In this case the quantity $c_{ij}\nabla n_i \cdot \nabla n_j$ is negligible since it is of the order of $(r_{ij}/L)^2$ compared to the local value of the homogeneous fluid free energy density f_o. Thus, it is appropriate to identify $\sum_{i,j} \frac{1}{2} c_{ij} \nabla n_i \cdot \nabla n_j$ as the free energy density of fluid microstructure.

Van der Waals introduced the one-component version of Equation (1) in his theory of liquid-vapor interfaces and Cahn and Hilliard[5,11] used a binary regular solution version of the equation in connection with interfacial structure and spinodal decomposition of subcooled homogeneous solution. In the modern statistical mechanical version of the theory,[2,6,7] Equation (1) is derived from a formal component density expansion of the exact free energy of inhomogeneous fluid. Expressions are obtained which relate the local "influence parameters" c_{ij} of inhomogeneous fluid to the fluid radial distribution functions of homogeneous fluid at local component densities. The heuristic connection of the influence parameter c_{ij} to $a_{ij}r_{ij}^2$ is justified by the rigorous statistical mechanical expressions.

In its modern version gradient theory is a very attractive description of inhomogeneous fluid: on the one hand the inputs $f_o(\underline{n})$ and $c_{ij}(\underline{n})$ can in principle be computed from the molecular theory of homogeneous fluid, but on the other hand if molecular theory is insufficiently developed for the fluids of interest semiempirical or empirical schemes can be used to deduce equations of state for $f_o(\underline{n})$ and $c_{ij}(\underline{n})$. Along these lines it is encouraging that the molecular theoretical formulas for c_{ij} and some predictions[12,13] based on simple models imply that the influence parameters are often only weak functions of component densities. Similarly, the success of the theory with constant c_{ij} in predicting the surface tensions of hydrocarbon mixtures[9] and water[10] argues against appreciable density dependence of the influence parameters. The importance of this is that one can determine the values of influence parameters from limited experimental data. In all the applications I discuss below the influence parameters are held constant.

At equilibrium the grand potential,

$$\Omega \equiv F - \sum_i \mu_i \int_V n_i d^3r \ , \qquad (2)$$

is a minimum in a closed system. The chemical potential, μ_i, plays the role of a Lagrange multiplier accounting for the constraint that $N_i (= \int n_i d^3r)$ is fixed in a closed system. The density distributions $n_i(\underline{r})$, $i=1,\cdots,\nu$, that minimize Ω must, according to the calculus of variations, obey the corresponding Euler equations

$$\mu_i = u_i^e + \mu_i^o(\underline{n}) - \sum_j \nabla\cdot(c_{ij}\nabla n_j) + \sum_{j,k} \frac{1}{2} \frac{\partial c_{jk}}{\partial n_i} \nabla n_j \cdot \nabla n_k \ ; \ \mu_i^o \equiv \partial f_o / \partial n_i \ , \qquad (3)$$

$i=1,\cdots,\nu$. Boundary conditions appropriate for a given fluid microstructure must be assigned and the component densities of the microstructure determined by solving these nonlinear differential equations. *Thus, gradient theory reduces the problem of determining equilibrium fluid microstructures to a nonlinear boundary value problem.* Of course, once a microstructure solution has been obtained its stability has to be established by proving that it is a local minimum of the grand potential Ω. Typically one solves nonlinear differential equations by discretization (e.g., finite difference or finite element) and iteration using the Newton-Raphson technique.[14,15] A biproduct of such a solution technique is that the matrix generated by the Newton-Raphson technique is the one required for stability analysis of the solution so obtained, i.e., the same algorithm generates the solution and the elements of stability analysis.

The pressure tensor is another quantity of interest in fluid microstructures. In homogeneous fluid, the pressure is isotropic, i.e., the number of lines of force passing through a small element of area from molecules lying on each side of element is independent of the orientation of the element. This is because the molecular population is identical in all directions in homogeneous fluid. This is not true in inhomogeneous fluid and so the isotropic pressure of homogeneous fluid, $P_o(n)\underline{I}$, must be corrected to account for local component density variation. $\underline{I}$ is the unit tensor. Since the number of lines of force passing through the area element will depend on orientation, components of the pressure tensor are in general different in an inhomogeneous fluid, i.e., the pressure tensor $\underline{P}$ is anisotropic. To second order in density gradients the general formula for the pressure tensor is of the form[2]

$$\underset{\sim}{P} = P_o(\underline{n})\underset{\sim}{I} + \sum_{i,j} \{\ell_{ij}^{(1)} n_i \nabla\nabla n_j + \ell_{ij}^{(2)} (\nabla n_i)(\nabla n_j) + [\ell_{ij}^{(3)} n_i \nabla^2 n_j + \ell_{ij}^{(4)} (\nabla n_i)\cdot(\nabla n_j)]\underset{\sim}{I}\} \quad , \quad (4)$$

where $\ell_{ij}^{(1)}, \cdots, \ell_{ij}^{(4)}$ are functions of the local composition $\underline{n}$. The one component version of Equation (5) was first proposed by Korteweg.[16] The theoretical formulas for the $\ell_{ij}^{(\alpha)}$ are much more complicated than that for the influence parameters.[2] Several simplified versions of the $\ell_{ij}^{(\alpha)}$ have been investigated.[13] The simplest of these is obtained by assuming that the influence parameters are constant and that the $\ell_{ij}^{(\alpha)}$ must be consistent with the constancy. The result is[2]

$$\underset{\sim}{P} = P_o(\underline{n})\underset{\sim}{I} - \frac{2}{3} \sum_{i,j} c_{ij}\{n_i \nabla\nabla n_j - \frac{1}{2}(\nabla n_i)(\nabla n_j) + \frac{1}{2}[n_i \nabla^2 n_j - \frac{1}{2}(\nabla n_i)\cdot(\nabla n_j)]\underset{\sim}{I}\} \quad . \quad (5)$$

Since f_o and P_o are related by the thermodynamic relation $dP_o = -d(f_o V)$, at constant $T, n_1 V, \cdots, n_\nu V$, the gradient theory of stress given by Equation (5) requires exactly the same inputs as the gradient theory of the free energy.

In what follows the influence parameters are always assumed to be constant and either the van der Waals (VDW) equation of state or one of its empirically modified successors, the Peng-Robinson (PR) equation,[17] is used. Both equations can be summarized as

$$P_o(\underline{n}) = \frac{nkT}{1 - nb} - \frac{n^2 a}{1 + \psi[2nb-(nb)^2]} \quad (6)$$

$\psi=0$ in the VDW equation and $\psi=1$ in the PR equation. a and b are energy and volume parameters. For pure fluids the parameters are determined by the critical temperature and pressure for the VDW equation and these plus the acentric factor for the PR equation.[17] The recommended forms of a and b for mixtures is $nb = \sum_i n_i b_i$ and $n^2 a = \sum_{i,j} n_i n_j a_{ij}$, where b_i and a_{ii} are pure fluid parameters and a_{ij}, $i \neq j$, are mixture parameters to be determined by a fit of the equation to experimental data on two-component systems. The PR equation is quantitatively superior to the VDW equation but qualitatively both are quite similar, and so either serves equally well the purposes of this article.

Planar interfaces

The component density profiles, $n_i(x)$, of a planar interface are obtained by solving Equation (3) with $u_e = 0$ and subject to the boundary conditions $\underline{n}(x = -\infty) = \underline{n}^{(1)}$ and $\underline{n}(x=\infty) = \underline{n}^{(2)}$, where $\underline{n}^{(1)}$ and $\underline{n}^{(2)}$ denote the component densities in coexisting bulk phases 1 and 2. These component densities are of course determined by the usual equilibrium conditions $P_o(\underline{n}^{(1)}) = P_o(\underline{n}^{(2)})$, $\mu_i^o(\underline{n}^{(1)}) = \mu_i^o(\underline{n}^{(2)})$, $i=1,\cdots,\nu$. Equation (3) can be solved analytically in the case of a one-component fluid but must be solved numerically in the multicomponent case.[6,9,18]

The density profile of a one-component liquid-vapor interface predicted with the VDW equation at the reduced temperature $kTb/a = 0.197$ is shown in Figure 1. The density is

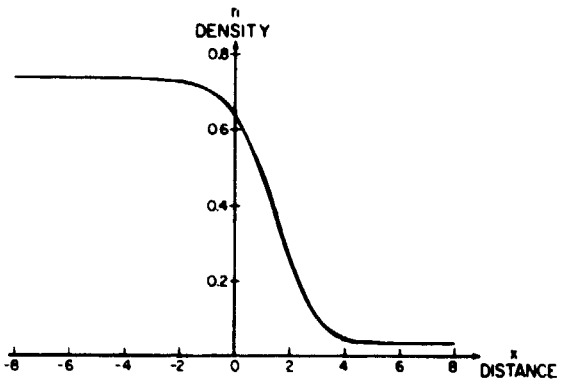

Figure 1. Density in units of b^{-1}, distance in $\sqrt{c/a}$. $kTb/a = 0.197$. Ref. 14.

given in units of b^{-1} and the distance in units of $\sqrt{c/a}$, a length of the order of magnitude of a molecular diameter. In a planar interface the normal pressure P_N, that is the component of pressure measured by a flat test surface lying in the interfacial plane, is constant in accordance with the condition of hydrostatic equilibrium ($\nabla \cdot P = 0$, or $dP_N/dx = 0$ since $P = P_N \hat{i}\hat{i} + P_T(\hat{j}\hat{j} + \hat{k}\hat{k})$, $\hat{i}$ the unit vector along the x-axis). On the other hand, the transverse pressure P_T, the component of pressure measured by a flat test surface orthogonal to the interfacial plane, is not constrained by hydrostatic equilibrium and must take on whatever values forced on it by the density profile. P_T cannot be constant in the interface; otherwise, the interfacial tension, which is the difference between the normal and transverse pressures integrated across the interface, namely,

$$\gamma = \int_{-\infty}^{\infty} (P_N - P_T)dx \ , \tag{7}$$

would have to be zero.

From Equation (5) it follows that

$$P_T = \frac{2}{3} P_o(n) + \frac{1}{3} P_N \ . \tag{8}$$

This result, which has been derived from several approximations[13] to the coefficients in the gradient theoretical pressure tensor, is heuristically very suggestive. The density $n(x)$ is uniform in a plane parallel to the interface, that is the pressure is isotropic in such a plane. The contribution to the transverse pressure from molecules lying near the plane is expected to be proportional to $P_o(n(x))$. Molecules lying further from the plane are distributed to maintain a constant normal pressure P_N. The contribution of the so-distributed molecules to the transverse pressure should be of same order of magnitude. Thus, it might be argued that P_T will be a linear combination of $P_o(n)$ and P_N, the respective coefficients being 2/3 and 1/3 reflecting the fact that the dimensions of the interfacial plane are 2 and the normal direction is 1. It would be interesting to find a convincing derivation of Equation (8) from this point of view. An accounting of the lines of intermolecular force passing through a small element of area versus orientation of the element might be fruitful in pursuing this goal.

An important implication of Equation (8) is that the structure of the transverse pressure in the interface is determined by the equation of state of homogeneous fluid. The normal and transverse pressures corresponding to the profile in Figure 1 are shown in Figure 2. As expected there is a wide region in which the interface is under tension (i.e., $P_T < P_N$). Since tension is positive and equals the area under the curve $P_N - P_T$ versus x, there must be a region in which $P_T > P_N$. There is however a small region of compression ($P_T > P_N$) on the gas side of the interface. The correspondence between the van der Waals loops in the PVT phase diagram for homogeneous fluid is seen by comparing Figures 2 and 3. The normal pressure P_N is of course the liquid-vapor coexistence pressure, i.e., $P_N = P_o(n_\ell) = P_o(n_g)$, n_ℓ and n_g the liquid and vapor densities, respectively. The region of compression in the interface arises from the region in which the pressure isotherm lies above the tie-lines, which locate the pressure P_N.

A significant feature of the theory is that the structure and stress in the interface are determined by the thermodynamic functions of homogeneous fluid in the metastable and unstable regions of the PVT diagram. It has usually been thought that in the unstable region of the phase diagram the thermodynamic functions are meaningless. Far from being meaningless, the behavior of these functions in this region is a determining factor of interfacial behavior. The gradient terms provide the necessary free energy to stabilize states that would be unstable in homogeneous fluid.[7]

As a critical point or a solution plait point is approached, the VDW loops in the pressure isotherm begin to flatten out and become symmetric about the tie-line, both patterns of which drive the tension towards zero. That tension goes to zero as a critical point is approached is well-known, but the mechanism of getting low tension by symmetrizing the VDW loops of the pressure isotherm is novel. Such an example is provided in Figure 4, in which is given density and pressure profiles of the liquid-liquid interface of carbon dioxide and decane.[19] The profiles were predicted with the PR equation using the mixture parameter values $a_{12} = \sqrt{a_{11}a_{22}}$ and $c_{12} = 0.9\sqrt{c_{11}c_{22}}$ and c_{ii} values fitted from pure fluid surface tension. The tension of the interface in Figure 4 is $\gamma = 0.6$ dyn/cm.

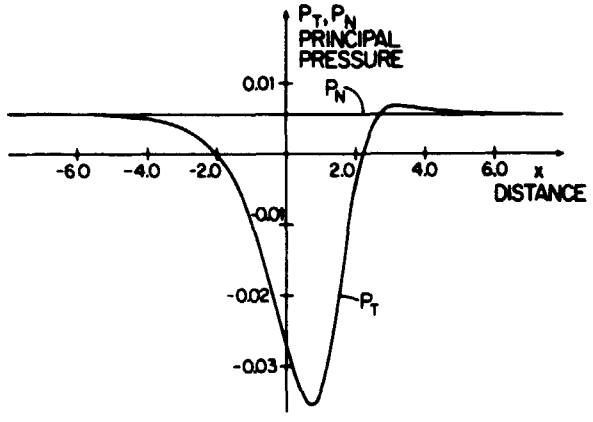

Figure 2. Principal pressures in a planar interface. VDW fluid. Pressure in units of a/b^2, distance in $\sqrt{c/a}$. Ref. 14.

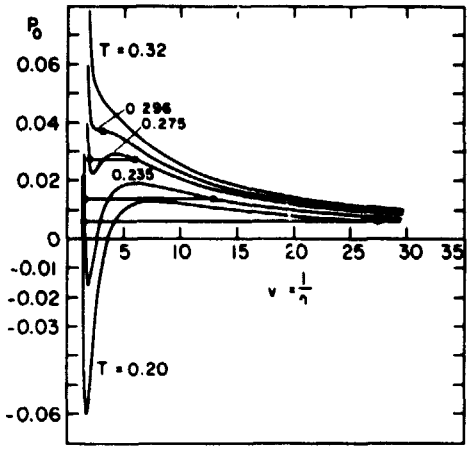

Figure 3. PVT phase diagram of a VDW fluid. Density in units of b^{-1} temperature in a/kb. The liquid-vapor densities are indicated by points connected with constant-pressure tie-lines.

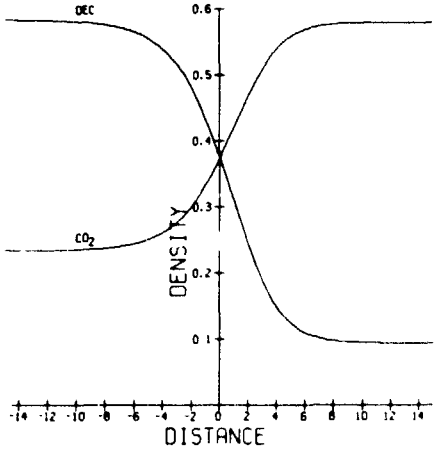

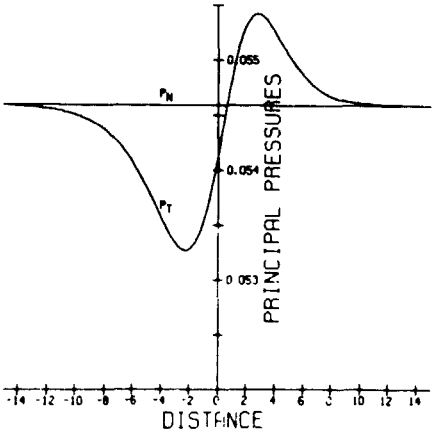

Figure 4. Density and principal pressure profiles of a CO_2-decane liquid-liquid interface of a PR fluid. $kTb/a = 0.148$, density n_i in units of b_i^{-1}, distance in $\sqrt{c/a}$, pressure in a/b^2. a, b, c CO_2 values. Ref. 19.

Contact angle, wettability, and film formation

The adsorption and wetting characteristics of fluids on solid surfaces and at fluid-fluid interfaces are of enormous practical interest in the design of detergents, lubricants, flotation and foaming agents, paints, capillary delivery devices, and the like. In spite of such practical importance, the molecular theory of adsorption and wetting is still a fledgling science, based most often on *ad hoc* models for various special situations. Gradient theory shows promise of giving a unified theoretical basis to the subject. In what follows, the theory is applied to adsorption and film formation at interfaces, three phase contact regions and the contact angle, and perfect wetting transitions.

Suppose a fluid-fluid interface contacts a flat solid wall as indicated in Figure 5. If the meniscus (a mathematical surface representing the position of the interface) is observed at some distance R lying far enough from the solid for bulk fluid phases to exist on each side of the surface but not far enough for gravitational distortion to affect it, then the observed contact angle θ obeys Young's equation

$$\gamma_{\gamma\alpha} = \gamma_{\gamma\beta} + \gamma_{\alpha\beta}\cos\theta \ . \tag{9}$$

$\gamma_{\gamma\alpha}$ and $\gamma_{\gamma\beta}$ denote the tensions (or surface excess free energies) of fluid phases α and β with solid phase γ. $\gamma_{\alpha\beta}$ is the interfacial tension of the interface between fluids α and β. The basis and meaning of Equation (9), which can be derived from a force balance on the hemicylinder whose cross-section is shown in dashed lines in Figure 5, has been discussed at length in a recent paper by Benner *et al.*[15]

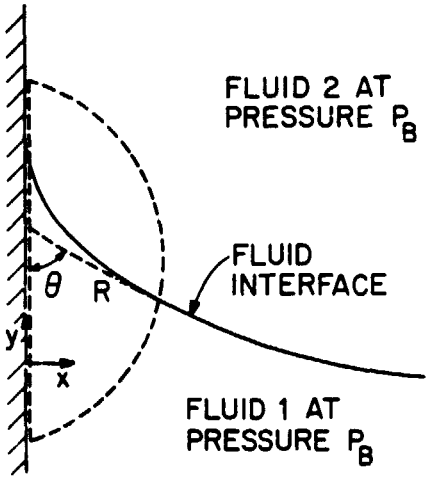

Figure 5. Angle of contact of fluid meniscus at a flat solid wall.

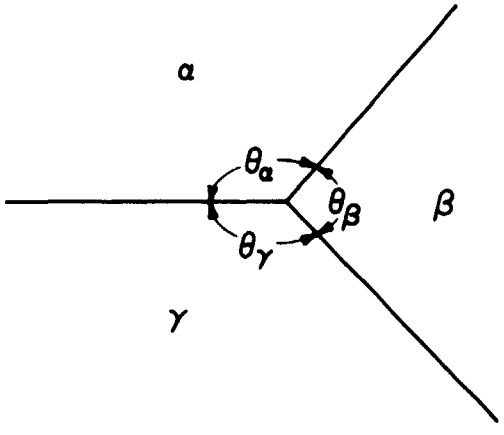

Figure 6. Angles of contact of three fluid phases.

If all three phase are fluid, then the menisci define three dihedral angles (Figure 6) obeying the force balance

$$\frac{\gamma_{\alpha\beta}}{\sin\theta_\gamma} = \frac{\gamma_{\gamma\beta}}{\sin\theta_\alpha} = \frac{\gamma_{\gamma\alpha}}{\sin\theta_\beta} \ . \tag{10}$$

A contact angle is not always observed when three phases are brought together. If either of the inequalities

$$\gamma_{\gamma\alpha} > \gamma_{\gamma\beta} + \gamma_{\alpha\beta} \qquad \text{or} \qquad \gamma_{\gamma\beta} > \gamma_{\gamma\alpha} + \gamma_{\alpha\beta} \tag{11}$$

then Equation (9) (or (10)) has no solution and the free energy of the system will decrease as the result of a thin layer of phase β (or phase α) intruding between phase γ and phase α (or phase β) as shown in Figure 7. The intruding phase is said to *completely or perfectly wet* the interface between the other two phases. The transition between contact angle and perfect wetting behavior occurs at conditions for which one of the inequalities in Equation (11) becomes an equality.

Perfect wetting is of course essential in applications involving spontaneous spreading of some fluid at an interface. Examples of perfect wetting are well-known. In the presence of air, most liquids perfectly wet on clean metal surfaces, water on quartz, some organic liquids on water, some organic liquids on some polymers, etc. Not so well-known is critical point wetting, a phenomenon hypothesized recently by Cahn.[20] He noted that according to critical point theory and experiment, as a critical point of phase α and β is approached along a temperature, pressure, or chemical potential path, the interfacial tension approaches zero asymptotically as

$$\gamma_{\alpha\beta} = \gamma^{o}_{\alpha\beta}\left|1 - \frac{h}{h_c}\right|^{1.3}, \qquad (12)$$

where h is the field variable (any thermodynamic quantity being the same in all coexisting phases), h_c its value at the critical point, and $\gamma^{o}_{\alpha\beta}$ a scale factor. Cahn postulated that the difference $|\gamma_{\gamma\alpha} - \gamma_{\alpha\beta}|$ will approach zero as the composition of the components in phases α and β approach each other, i.e., it obeys the scaling law

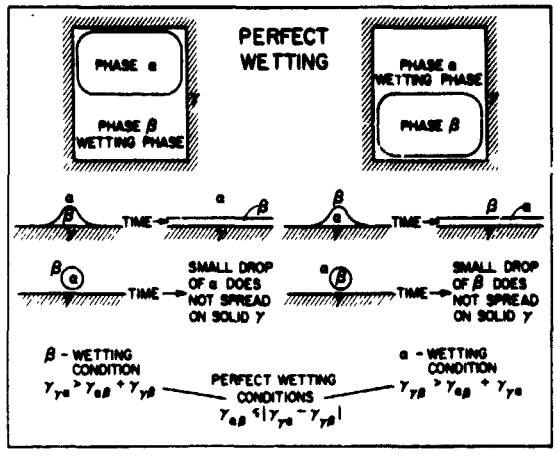

Figure 7. Conditions for perfect wetting by either phase α or phase β.

$$\left|\gamma_{\gamma\alpha} - \gamma_{\alpha\beta}\right| = \gamma^{o}_{\alpha\beta\gamma}\left|1 - \frac{h}{h_c}\right|^{0.34} \qquad (13)$$

sufficiently near the critical point. Since $\gamma_{\alpha\beta}$ approaches zero faster than that postulated for $|\gamma_{\gamma\alpha} - \gamma_{\gamma\beta}|$, Cahn concluded that there will always exist a critical wetting value of the field variable, h_{cw}, not equal to h_c, at which one of the fluids will become perfectly wetting. The combination of Equations (9), (12) and (13) gives asymptotic formulas for the contact angle at a solid as h approaches h_{cw}, namely,

$$\cos\theta = \pm\left(\frac{\gamma_c}{\gamma_{\alpha\beta}}\right)^{0.74} = \pm\left|\frac{h_{cw} - h_c}{h_c - h}\right|^{0.96} \qquad (14)$$

where γ_c is the value of $\gamma_{\alpha\beta}$ at $h = h_{cw}$.

The practical significance of Cahn's theory is that one of a pair of fluids can always be made perfectly wetting in the presence in a third phase by adjusting field variables (e.g., by changing temperature or pressure or by adding some component) to get near a critical point.

To test the validity of Equation (13), an unverified hypothesis, and to understand the relation of γ_{cw} and h_{cw} to fluid and solid properties and interfacial structure, Teletzke *et al.*[21] studied with gradient theory the behavior of a one-component fluid at a flat solid wall. Some results of this work are of interest here. The PR equation of state was used for the fluid and the wall was characterized by the wall-fluid molecule potential

$$u_e(x) = W\left[\frac{1}{45}\left(\frac{d}{x}\right)^9 - \frac{1}{6}\left(\frac{d}{x}\right)^3\right], \qquad (15)$$

a choice appropriate for walls and fluids composed of molecules interacting with the 6-12 Lennard-Jones potential. x denotes the distance from the wall. W is a measure of the strength of the wall-fluid potential and d its range.

The gradient profile equation with constant influence parameter was solved for the density profile n(x) by the Galerkin technique using a finite element basis set. The solid-fluid tension can be computed as the area derivative of the free energy, $\gamma = \partial F/\partial A$, or, equivalently, from the pressure formula, $\gamma = \int_0^\infty [P_o(n_B) - P_T]dx$, n_B being the bulk density of fluid far from the wall. The boundary conditions for the problem are $n(x)\to 0$ as $x\to 0$ and $n(x)\to n_B$ as $x\to\infty$.

A PR fluid has an upper critical temperature T_c equal to 0.1704 in the units a/b.

Gradient theory predicts a critical-wetting temperature T_{cw} above which the liquid phase becomes perfectly wetting at the solid-vapor surface. An example is shown in Figure 8, for the solid-fluid parameters $W = 6.4\ a/b$ and $d = \sqrt{c/a}$. Below T_{cw} a drop of liquid would not spread on the solid, but would form a contact angle. Above T_{cw} the drop would spread to form a perfectly wetting layer. The critical wetting temperature depends on W and d. At fixed d, T_{cw} decreases with increasing W, i.e., as the strength of the solid-liquid potential increases perfect wetting occurs at lower temperature. At fixed W, T_{cw} decreases with increasing range d of the wall potential, i.e., the longer the range of the potential the lower the temperature at which perfect wetting occurs.

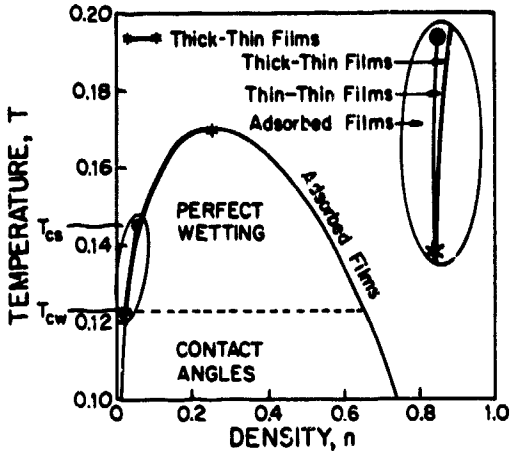

Figure 8. Phase and film diagram for a Peng-Robinson fluid. Temperature in units a/kb, density in b^{-1}. Ref. 21.

Correspondingly, the characteristic tension $\gamma_c \equiv \gamma_{LV}(T_{cw})$ decreases with increasing T_{cw} (and, therefore, with decreasing W or d). If W and/or d are small enough, then T_{cw} is near the critical point and Equation (14) should hold if Cahn's hypothesis is true. This was indeed found to be true (although there is a small detail of mean-field versus correct scaling laws[21]). On the other hand, as W and/or d increase, the perfect-wetting temperature T_{cw} decreases and Equation (14) no longer holds. At sufficiently low temperature the interface is very sharp (narrow) and the Good-Girifalco formula[23]

$$\cos\theta = 2\sqrt{\frac{\gamma_c}{\gamma_{LV}}} - 1 \tag{16}$$

ought to hold since it is based on a discontinuous interface approximation. This turns out to be the case. The dependence of T_{cw} and $\gamma_c = \gamma_{LV}(T_{cw})$ on W and the dependence of $\cos\theta$ on $\gamma_{LV}(T)/\gamma_c$ for various values of W are shown in Figures 9 and 10 for the case $d = \sqrt{c/a}$. The

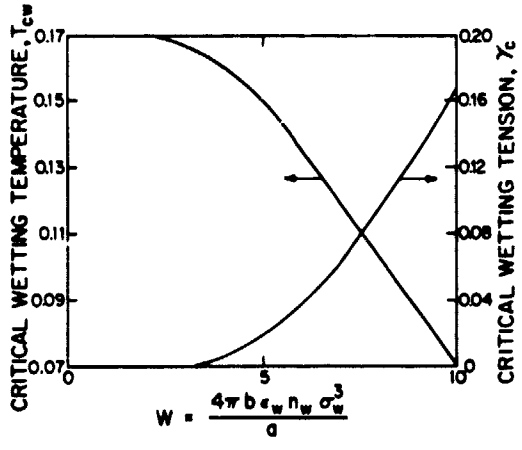

Figure 9. Variation of critical wetting temperature (units a/kb) critical wetting tension (units $\sqrt{ac}/b^2$) with W (units a/b). Ref. 21.

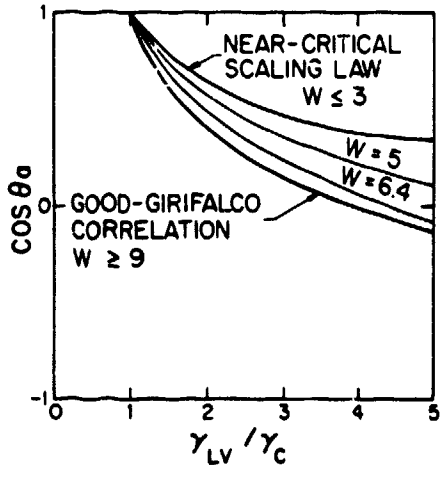

Figure 10. Contact angle versus $\gamma_{LV}(T)/\gamma_c$ for various W. Ref. 21.

near-critical scaling law, Equation (14), holds for $W \leq 3$, the Good-Girifalco formula, Equation (16), holds for $W \geq 9$. In the intermediate range, neither formula holds.

Several years ago, Zisman[24] suggested that the contact angle correlates with the ratio γ_{LV}/γ_c but that γ_c was a characteristic only of the solid, not of the fluid phase. The implication of Figure 9 is that this is not so unless the reduced energy parameter Wb/a and length parameter $d/\sqrt{c/a}$ are fixed in the series of fluids compared. As these ratios depend both on solid and fluid, it appears that Zisman's scaling worked because the fluid parameters b/a and $\sqrt{c/a}$ were not very different for the systems compared.

Another thing gradient theory predicts is a first order transition of the absorbed layer at the solid surface. In the temperature range T_{cw} to T_{cs} (Figure 8), as the bulk fluid density increases from zero towards the gas side of the phase diagram a composition is reached at which two adsorbed layers or thin-films of different thickness are predicted at the same equilibrium conditions. An example is shown in Figure 11. As the bulk density is increased beyond the thin-film coexistence curve the thin-film grows continuously into a thick thin-film to become finally a perfectly wetting layer of liquid when the liquid-vapor phase dome is reached. The temperature T_{cs} is a film critical point. Above T_{cs}, as bulk density increases from zero to the liquid-vapor coexistence curve an adsorbed layer grows continuously through thin-film states into a perfectly wetting layer of liquid phase. Below T_{cw} only submonolayer adsorption occurs with increasing density until at the liquid-vapor coexistence curve liquid appears as a drop with a contact angle. On the liquid side of the coexistence region only submonolayer adsorption occurs. A thin-film transition was predicted by Saam and Ebner[25] using an integral model free energy. Their thin-film coexistence curve is very similar to that of described here. The thin-film transition predicted by Cahn on the basis of a two-dimensional model of the solid is, however, qualitatively different.[21]

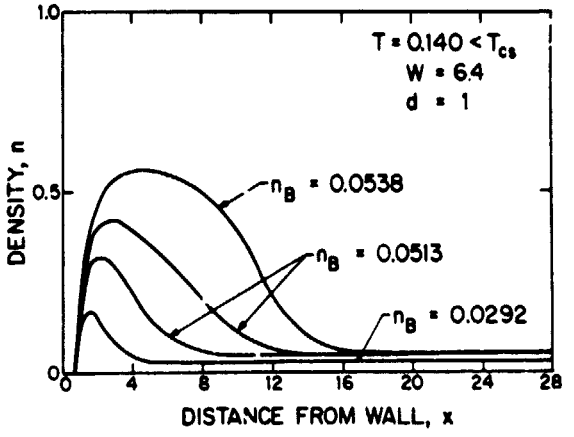

Figure 11. Density profile of fluid at a solid wall as a function of bulk fluid density. Ref. 21.

It should be emphasized that according to the theory the patterns of film and phase behavior of a one-component fluid at a solid wall are general. Sufficiently near a critical point of a pair α and β of multicomponent coexisting fluid phases, either α or β will become perfectly wetting at the interface formed by a third phase γ and the nonwetting fluid phase. The third phase γ can be solid or liquid. The critical point can be an upper or lower critical point. In approaching a critical point along any field variable h, e.g. temperature, pressure, or chemical potential of a component, there will be a critical wetting value h_{cw}, a finite distance from the critical point value h_c, at which one of the near-critical phases becomes perfectly wetting on a third phase. Outside but near the coexistence composition region of α and β, a first order thin-film transition occurs with a coexistence curve lying between h_{cw} and h_{cs}, h_{cs} being the film critical point. h_{cs} lies between h_{cw} and h_c. If h lies between h_{cw} and h_c, then sufficiently near the α-β coexistence region a thin-film formed between the third phase γ and, say, phase α will thicken continuously into a layer of the perfectly wetting phase β.

An example of the structure and stress of a liquid-vapor interface at which a thin-film has almost grown into a layer of a second liquid phase is shown in Figure 12. This figure was taken from the work of Falls *et al.*[19] in which theory was applied with the PR equation to planar interfaces and spherical drops formed in carbon dioxide and decane mixtures. The transverse pressure profile is highly structured, looking like that of a liquid-liquid interface on the left and of a liquid-vapor interface on the right.

There is abundant evidence that the qualitative patterns of wetting transitions described ere are correct[26,22,27] and the expected continuously thickening thin films have been observed by ellipsometry.[28] However, the predicted first order thin-film transition has not been verified experimentally, nor have the critical exponents of Equations (13) and (14) been established experimentally.

The theory of wetting transitions and film formation at flat surfaces requires solving only a one-dimensional density profile problem. However, if the structure and stress of

Corrective Page

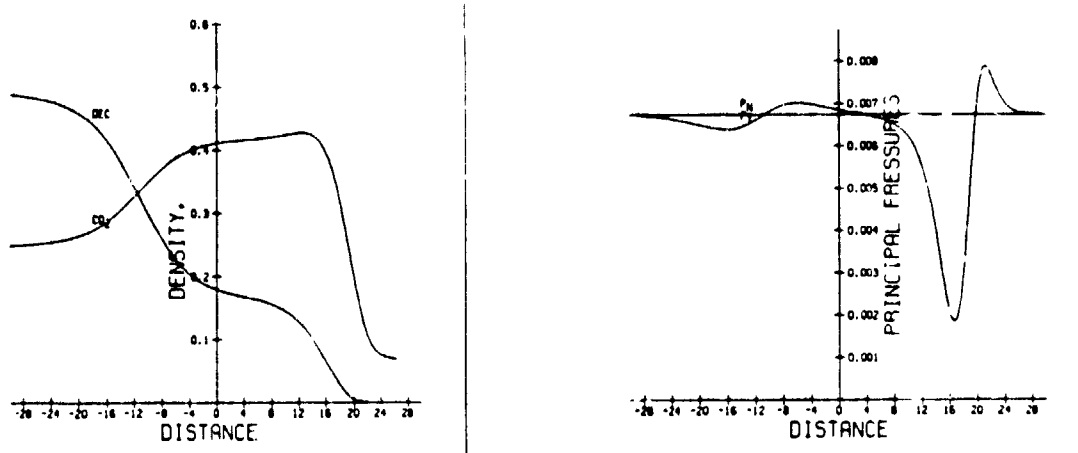

Figure 12. Density and pressure profiles of a thin-film at a liquid-vapor interface in CO_2 and decane. Density n_i in units b_i^{-1}, distance in $\sqrt{c_{11}/a_{11}}$ and pressure in a_{11}/b_1^2. Component 1 is CO_2. $kTb_1/a_{11} = 0.148$. Ref. 19.

the three phase contact region is desired, the problem becomes of necessity greater than one-dimensional, even if one phase is a flat solid. If a fluid-fluid interface contacts a flat solid the component densities depend on the distance x from the wall and the distance y parallel to the wall. Benner *et al.*[15] have recently studied the contact region of a one-component liquid-vapor interface at flat solid. The PR equation was used for the fluid and Equation (15) for the wall-fluid interaction potential. The space available here does not allow an extensive discussion of the paper. However, one interesting feature is that the stress state in the liquid-vapor interface is affected relatively far from the interface. An example of this is given in Figure 13. The principal pressure directions in the x-y plane are indicated by crosses, the size of which indicates the magnitudes of the principal pressures in the x-y plane. Far away from the solid and the liquid-vapor meniscus (defined as the position where $n(x,y) = 1/2(n_g + n_\ell)$ and indicated by the solid curve) the pressure components equal the bulk fluid value wich is so small the corresponding crosses are almost invisible on the scale of Figure 13. At a planar liquid-vapor interface the normal pressure component (P_{11}) would be constant and therefore the pressure crosses would appear as horizontal lines (P_{22} large, P_{11} small) in the interfacial zone. Instead, even to the far right of Figure 13, a distance of about 25 molecular diameters away from the wall, the normal pressure component is very large. And the principal stress pairs P_{11}, P_{22} undergo four sign changes in going from the liquid to the vapor phase. Wild and wonderful patterns! Are they consequential? A major conclusion from the work of Benner *et al.* is that at a flat surface Young's equation is applicable outside the contact region (see Figure 5). The radius of the contact region is two or three times the thickness of the interfacial zone between the fluid phases.

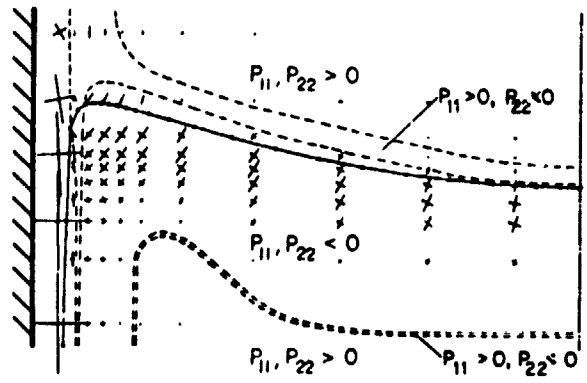

Figure 13. Principal pressure and components in a liquid-vapor interface near a wall. $kTb/a = 0.1$, $W = 6a/b$. Width of region shown is $25\sqrt{c/a}$. PR fluid. Ref. 15.

Spherical fluid microstructures

Visible examples of spherical microstructures are the drops and bubbles that occur in mists, foams, beverages, manufactured glass, and basalt lavas. Invisible examples are colloidal particles, vesicles, and micelles. The classical description of spherical structures is based on the Young-Laplace equation and the Kelvin equation expressing mechanical and chemical equilibrium between a bulk phase interior and a bulk phase exterior separated by an interface having the tension of a planar interface. In a sufficiently small spherical microstructure, however, the interior will not be bulk phase and the tension will not be that of a planar interface. Deviation from classical behavior might be consequential in nucleating fluids and micellar solutions, in which the equilibrium microstructures are tens of angstroms in diameter and, to mention a couple of examples receiving special attention at this colloquim, microdrops or microbubbles in microdrops and thin liquid layers on the inside of glass shells.

Gradient theory provides a molecular level theory of spherical structures which establishes the point at which the classical description breaks down and determines the structure, stress and mechanisms of stability of spherical microstructures. By way of example, I will outline some results of the recent investigations of Falls *et al.*[14,19] on one and two-component microdrops and microbubbles.

For spherical microstructures suspended in bulk fluid, the boundary conditions are $\partial n_i/\partial r = 0$ at $r=0$ and $n_i(r) \rightarrow n_{iB}$ as $r \rightarrow \infty$, n_{iB} being the bulk phase density of i in the suspending fluid. With these boundary conditions and constant influence parameters, Falls *et al.* have solved gradient theory for a one-component VDW fluid[14] and a two-component PR fluid.[19] Figure 14 illustrates their results for the density profiles n(r) of liquid-like microdrops suspended in a vapor phase. From the Young-Laplace and Kelvin equations, one expects the interior of the drop to be at higher pressure, and therefore higher density, than the saturated liquid density n_i^{eq}. This is seen to be true in Figure 14 for drops of radius larger than about four molecular diameters (the "radius" of the drop does not have a precise meaning for microdrops). However, for smaller drops, the interior density decreases with drop size and the density profile takes on a Gaussian-like shape with no interior bulk region. The loss of a bulk-like interior begins to occur when the radius of the drop is about equal to the thickness of the liquid vapor interface.

Because the interface is curved, the normal pressure profile P_N ($\underset{\approx}{P} = P_N(r)\hat{r}\hat{r} + P_T(r)(\underset{\approx}{I} - \quad)$ in a spherical fluid structure) is not constant across the interface. Thus, the pressure profiles in a spherical interface are quite different from those in a planar interface at the same temperature (compare Figures 15 and 2). This leads one to expect strong deviations between the tension γ_∞ of a planar interface and the tension $\gamma(R)$ of a microdrop of radius R. Similar deviations are expected for the Young-Laplace equation as classically applied, i.e. $P_N(r=0) - P_N(r=\infty) = 2\gamma_\infty/R$. From the thermodynamics of drops it follows that the appropriate radius R with which to describe the tension of the drop is the radius of the surface of tension.[29] This radius (which does not differ greatly from the value of r at which $n(r) = 1/2(n(r=0) + n_B)$) and the corresponding tension $\gamma(R)$ are predicted by gradient theory.[14] As illustrated in Table 1, the tension of the drop does differ from γ_∞ for small drops and the classical Young-Laplace equation does break down. However, what is remarkable is that already for drops fifteen molecules wide the drop interface has virtually the same tension as a planar interface and the classical Young-Laplace equation is accurate.

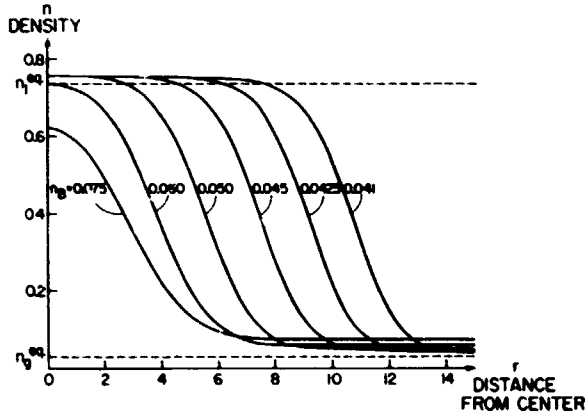

Figure 14. Density profiles of microspherical drops in a VDW vapor. $kTb/a = 0.197$, density in units of b^{-1}, distance $\sim \sqrt{c/a}$.

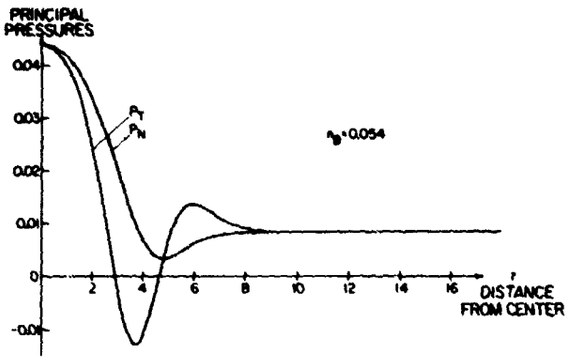

Figure 15. Principal pressure profiles of a microspherical drop in a VDW vapor. Pressure in units of a/b^2, density in b^{-1}, distance in $\sqrt{c/a}$. $kTb/a = 0.197$. Ref. 14.

Table 1. Microdrops in VDW vapor. Radius R in units of $\sqrt{c/a}$. $kTb/a = 0.197$.

R	$\gamma(R)/\gamma_\infty$	$\frac{P_N(0) - P_N(\infty)}{(2\gamma_\infty/R)}$
2.56	0.79	-0.079
2.88	0.83	0.017
3.26	0.87	0.19
3.76	0.91	0.43
4.62	0.95	0.73
5.52	0.97	0.87
7.74	0.99	0.97
10.15	0.996	0.99

The implication of the one-component studies just outlined is that microdrop curvature affects the interfacial structure and the interfacial tension very little once the drop radius is larger than 10 molecular diameters. In multicomponent systems this conclusion may or may not follow. Consider for example the bubble in liquid CO_2 and decane shown in Figure 16 (from Falls *et al.*[19]). The radius of the bubble is only about 12 carbon dioxide diameters, but its component density profiles are almost identical to those of the planar liquid vapor interface (indicated as a bubble with R=∞).

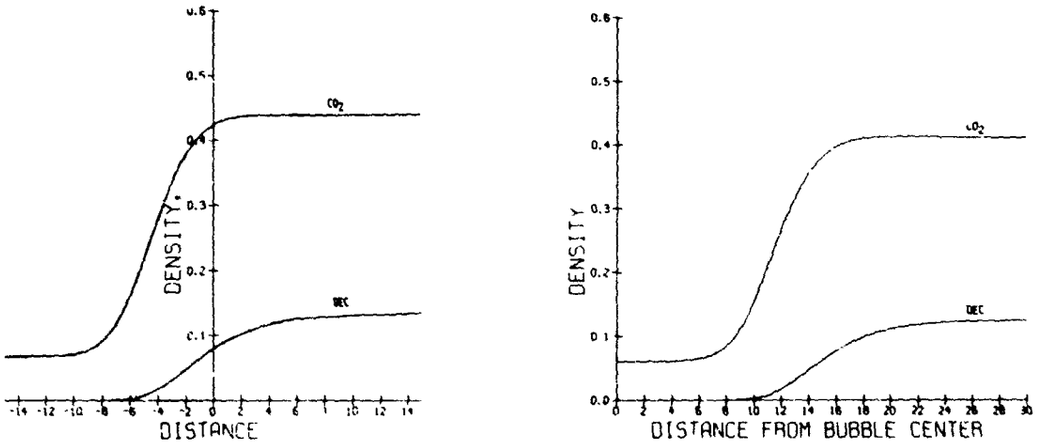

Figure 16. Density profiles in a planar liquid-vapor interface (R=∞) and in a bubble (R = 12) in a CO_2-decane PR fluid. Density n_i in units of b_i^{-1}, distance in $\sqrt{c_{11}/a_{11}}$. $kTb_1/a_{11} = 0.148$. Ref. 19.

The tensions of the bubble and planar interface agree within 10%. Thus, this bubble behaves as expected from the one-component results.

However, as was discussed in the previous section (Figure 12), in a multicomponent fluid conditions can be such that a thin-film of an incipient third phase may be formed at an interface. These films are very sensitive to a change in a field variable. Curving an interface changes the chemical potential of the system (this follows from Kelvin's equation in the classical theory), and so it can be anticipated that under conditions of high adsorption or thin-film formation the interfacial structure and stress will be very sensitive to drop size. Comparison of the drop component density and pressure profiles of Figure 17 (from Falls *et al.*[19]) with the corresponding planar case, Figure 12, illustrates that this is

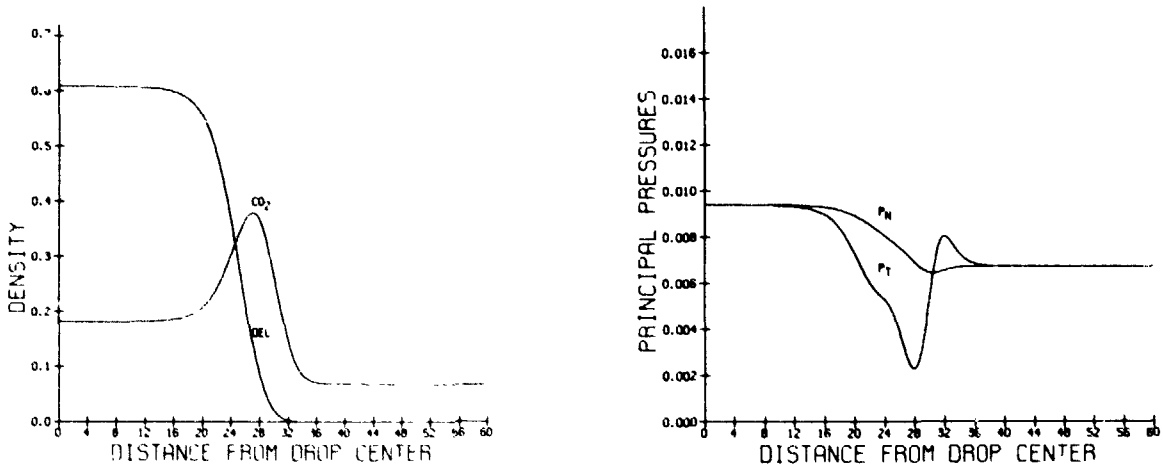

Figure 17. Density and pressure profiles of a drop in a CO_2-decane PR fluid. Density n_i in units of b_i^{-1}, pressure in a_{11}/b_1^2, distance in $\sqrt{c_{11}/a_{11}}$. $kTb_1/a_{11} = 0.148$. Ref. 19.

indeed the case. At this temperature, it has been estimated[19] from the theory that the drop structure will not begin take on the planar form until it is larger than 100 carbon dioxide molecules in radius. The important implication of this result is that *in regions of thin-film formation the interfacial composition can be greatly modified by curvature.* This fact might be quite important in the manufacture of objects with thin, uniform layers of a desired material.

Although space does not allow discussion, gradient theory predicts the work of formation of drops and bubbles, a quantity important to the theory of homogeneous nucleation. In fact, the theory was used by Cahn[11] to support his theory of spinodal decomposition. He showed that the barrier expected for the nucleation of microdrops is not there owing to the size dependence of the interfacial tension and that as a result a homogeneous material at the spinodal density can transform continuously into a multiphase system. In heterogeneous nucleation, it is likely that thin-film formation will be an important intermediate step in the process when conditions are right. These matters are ripe for future work.

Closing remarks

In closing, I would like the point out a few problems to which gradient theory might profitably be applied next.

1. Thin, uniform layers of fluid in a spherical solid shell. A fluid-solid potential will have to be introduced for shell. For uniform thin-films and thin layers of phase only spherically symmetric solutions need to be sought, so the problem remains one dimensional. By a different method Kim, Mok, and Bernat address this problem in their paper.
2. Fluid microstructure at rough or chemically heterogeneous solid surfaces. For this problem a two-dimensional solid-fluid potential will have to be introduced. Thus, the problem is two-dimensional.
3. Contact angles with rough or chemically heterogeneous solid surfaces. This involves the same solid-fluid potential as in Problem 2 and a fluid interface in the vicinity of

the solid and so is a three-dimensional problem. The problem will pose a challenge to computer-aided mathematics.

4. Drop shapes on inclined rough or chemically heterogeneous surfaces. This again is a three-dimensional problem and an even greater challenge than Problem 3.

Acknowledgement

I am grateful to the Department of Energy for financial support of this research and to my Minnesota colleagues for their roles in the research reviewed.

References

1. For example, see Percus, J. K., in The Equilibrium Theory of Classical Fluids, H. L. Frisch and J. L. Lebowitz, Eds., Benjamin, New York, 1966, pp. II33-II70.
2. For a recent review, see Davis, H. T. and L. E. Scriven, Advances in Chemical Physics, to appear early in 1982.
3. Lord Rayleigh, Phil. Mag. 33, 208 (1892).
4. Van der Waals, J. D. and Ph. Kohnstamm, Lehrbuch der Thermodynamik, Maas and Van Suchtelen, Leipzig, 1908.
5. Cahn, J. W. and J. E. Hilliard, J. Chem. Phys. 28, 258 (1958).
6. Bongiorno, V., L. E. Scriven and H. T. Davis, J. Colloid and Interface Sci. 57, 462 (1976).
7. Yang, J. M., P. D. Fleming III and J. H. Gibbs, J. Chem. Phys. 64, 3732 (1976).
8. Poser, C. I. and I. C. Sanchez, J. Colloid and Interface Sci 69, 539 (1979).
9. (a) Carey, B. S., L. E. Scriven and H. T. Davis, Am. Inst. Chem. Eng. J. 24, 1076 (1978); 26, 705 (1980). (b) Carey, B. S., Ph.D. Thesis, University of Minnesota, 1979.
10. Guerrero, M. and H. T. Davis, Ind. Eng. Chem. Fundam. 19, 309 (1980).
11. Cahn, J. W., J. Chem. Phys. 42, 93 (1965).
12. McCoy, B. F. and H. T. Davis, Phys. Rev. A 20, 1201 (1979).
13. Carey, B. S., L. E. Scriven and H. T. Davis, J. Chem. Phys. 69, 5040 (1978).
14. Falls, A. H., L. E. Scriven and H. T. Davis, J. Chem. Phys. 75, 3986 (1981).
15. Benner, R. E., L. E. Scriven and H. T. Davis, Royal Society of Chemistry's Faraday Symposium No. 16, "Structure of the Interfacial Region," Oxford University, 16-17 December 1981.
16. Korteweg, D. J., Archives Neerl. Sci. Exacts Nat. 6, 1 (1904).
17. Peng, D. Y. and D. B. Robinson, Ind. Eng. Chem. Fundam. 15, 59 (1976).
18. Sahimi, M., L. E. Scriven and H. T. Davis, 56th Annual Fall Technical Conference of SPE of AIME, San Antonio, TX, Oct. 5-17, 1981, SPE Reprint #10268.
19. From Falls, A. H., L. E. Scriven and H. T. Davis, J. Chem. Phys. (to be submitted).
20. Cahn, J. W., J. Chem. Phys. 66, 3667 (1977).
21. Teletzke, G. F., L. E. Scriven and H. T. Davis, J. Colloid and Interface Sci. (to appear).
22. Teletzke, G. F., L. E. Scriven and H. T. Davis, 56th Annual Fall Technical Conference of SPE of AIME, San Antonio, TX, Oct. 5-17, 1981, SPE Reprint #10112.
23. Good, R. J. and L. A. Girifalco, J. Phys. Chem. 64, 561 (1960); 61, 904 (1957).
24. Zisman, W. A., Adv. in Chem. Series 43, 1 (1963).
25. Saam, W. F. and C. Ebner, Phys. Rev. A 17, 1768 (1978).
26. Moldover, M. R. and J. W. Cahn, Science 207, 1073 (1980).
27. Teletzke, G. F., Ph.D. Thesis, University of Minnesota, 1[illegible]
28. Kwon, O.'D., D. Beaglehole, W. W. Webb, B. Widom, J. W. [illegible]dt, J. W. Cahn, M. R. Moldover and B. Stephenson (private communication).
29. Hill, T. L., J. Chem. Phys. 20, 141 (1952); J. Phys. Chem. 56, 526 (1952).